View metadata, citation and similar papers at core.ac.uk

brought to you by CORE

provided by University of Queensland eSpace

Accepted Manuscript

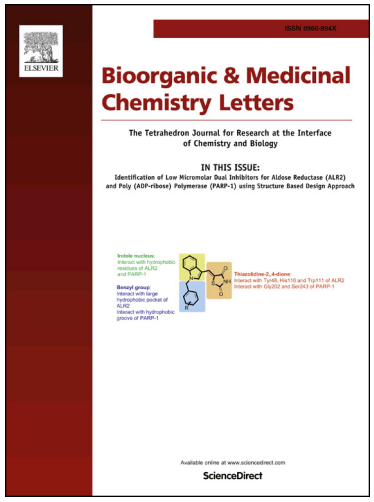

Quinazolinone derivatives as inhibitors of homologous recombinase RAD51

Ambber Ward, Lilong Dong, Jonathan M. Harris, Kum Kum Khanna, Fares Al-Ejeh, David P. Fairlie, Adrian P. Wiegmans, Ligong Liu

PII: S0960-894X(17)30520-6
DOI: http://dx.doi.org/10.1016/j.bmcl.2017.05.039
Reference: BMCL 24984

To appear in: *Bioorganic & Medicinal Chemistry Letters*

Received Date: 20 March 2017
Revised Date: 8 May 2017
Accepted Date: 13 May 2017

Please cite this article as: Ward, A., Dong, L., Harris, J.M., Khanna, K.K., Al-Ejeh, F., Fairlie, D.P., Wiegmans, A.P., Liu, L., Quinazolinone derivatives as inhibitors of homologous recombinase RAD51, *Bioorganic & Medicinal Chemistry Letters* (2017), doi: http://dx.doi.org/10.1016/j.bmcl.2017.05.039

This is a PDF file of an unedited manuscript that has been accepted for publication. As a service to our customers we are providing this early version of the manuscript. The manuscript will undergo copyediting, typesetting, and review of the resulting proof before it is published in its final form. Please note that during the production process errors may be discovered which could affect the content, and all legal disclaimers that apply to the journal pertain.

ACCEPTED MANUSCRIPT

ELSEVIER

Bioorganic & Medicinal Chemistry Letters
journal homepage: www.elsevier.com

Quinazolinone derivatives as inhibitors of homologous recombinase RAD51

Ambber Ward[a], Lilong Dong[b], Jonathan M. Harris[c], Kum Kum Khanna[d], Fares Al-Ejeh[a], David P. Fairlie[b,e], Adrian P. Wiegmans[a,f*] and Ligong Liu[b,e*]

[a] *Personalised Medicine, QIMR Berghofer Medical Research Institute, Herston Rd, Herston, Brisbane, Queensland, Australia*
[b] *Division of Chemistry and Structural Biology, Institute for Molecular Bioscience, The University of Queensland, Brisbane, Queensland, Australia*
[c] *School of Life Science, Queensland University of Technology, Brisbane, Queensland, Australia*
[d] *Signal Transduction Laboratory, QIMR Berghofer Medical Research Institute, Herston Rd, Herston, Brisbane, Queensland, Australia*
[e] *Australian Research Council Centre of Excellence in Advanced Molecular Imaging, Institute for Molecular Bioscience, The University of Queensland, Brisbane, Queensland, Australia.*
[f] *Tumour Microenvironment Laboratory, QIMR Berghofer Medical Research Institute, Herston Rd, Herston, Brisbane, Queensland, Australia*

* Corresponding Authors: +61 733620102, E-mail: adrian.wiegmans@qimrberghofer.edu.au; or +61 733462990, l.liu@imb.uq.edu.au.

Abbreviations: BRAC2, breast cancer type 2 susceptibility protein; GFP, green fluorescent protein; HR, homologous recombination; HTS, high throughput screening.

ARTICLE INFO

Article history:
Received
Revised
Accepted
Available online

Keywords:
Homologous recombination
DNA repair
RAD51
Inhibitor
Triple-negative breast cancer

ABSTRACT

RAD51 is a vital component of the homologous recombination DNA repair pathway and is overexpressed in drug-resistant cancers, including aggressive triple negative breast cancer (TNBC). A proposed strategy for improving therapeutic outcomes for patients is through small molecule inhibition of RAD51, thereby sensitizing tumor cells to DNA damaging irradiation and/or chemotherapy. Here we report structure-activity relationships for a library of quinazolinone derivatives. A novel RAD51 inhibitor (**17**) displays up to 15-fold enhanced inhibition of cell growth in a panel of TNBC cell lines compared to compound B02, and approximately 2-fold increased inhibition of irradiation-induced RAD51 foci formation. Additionally, compound **17** significantly inhibits TNBC cell sensitivity to DNA damage, implying a potentially targeted therapy for cancer treatment.

2009 Elsevier Ltd. All rights reserved.

RAD51 is the essential recombinase in the homologous recombination (HR) repair pathway, one of two cellular pathways that repair double-strand DNA (dsDNA) breaks [1]. Upregulation of RAD51 is reported in several cancers, including triple-negative breast cancer (TNBC) [2], glioblastoma [3], prostate cancer [4], and is a mechanism by which these tumors acquire resistance to therapies. HR-defective cells are significantly more sensitive to ionizing irradiation and DNA damaging chemotherapeutics [1]. Since the pathway is predominantly utilized by actively replicating cells, short-term disruption of HR has little impact on quiescent cells of normal tissue, whilst being detrimental to rapidly proliferating cancer cells [1].

RAD51 has been recognized as a potential oncotarget due to its critical role in HR, and contributes to an aggressive cellular phenotype and resistance to therapeutics. Several small molecule RAD51 inhibitors have been discovered by high-throughput screening of compound libraries, notably B02 [5-7], the RI series [8-10] and the IBR2 series [11,12] (Figure 1). Alternatively, a fragment-based screening approach at Cambridge identified another series of compounds [13,14] (Figure 1). Mechanistically, B02 disrupts RAD51 binding to ssDNA, RI-1 interferes with RAD51 binding to dsDNA, and IBR2 and the Cambridge series inhibit RAD51-BRCA2 interaction. These compounds have cytotoxic activity at micromolar concentrations.

B02 was the first of these compounds to be well-profiled [7]. DNA binding assays revealed that it disrupted initial RAD51 binding to ssDNA, and later dsDNA binding to the RAD51-ssDNA filament [7]. A D-loop assay confirmed B02 specificity for human RAD51 over its bacterial homologue RecA and other human HR proteins[15]. *In vitro*, B02 inhibited irradiation-induced RAD51 foci formation, HR repair of dsDNA breaks [7] and sensitized cells to a panel of chemotherapy drugs [5,7]. *In vivo* B02 significantly enhanced the therapeutic effect of cisplatin in a TNBC xenograft model[5]. The structure of B02 involves three chemically distinct components, which could be constructed and optimised through parallel approaches. Here we describe some structure-activity relationships for analogues of B02, leading to the discovery of an inhibitor selective for several human breast cancer cell lines including those expressing high RAD51.

ACCEPTED MANUSCRIPT

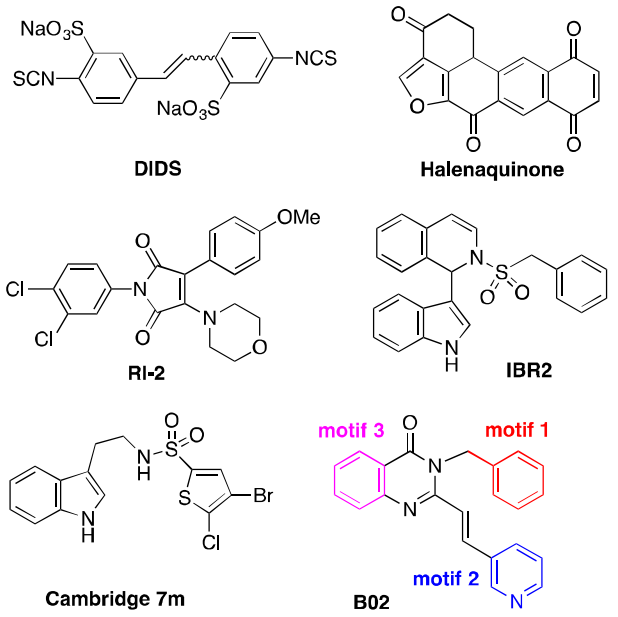

Figure 1. Structurally different RAD51 inhibitors, including B02. Components of B02 to be varied in this study are separately colored.

Several years ago, we developed a homology model of human RAD51, based on a full-length homologue from *Pyrococcus furiosus* (PDB code: 1PZN [16]), to aid compound design. B02 was docked into the model in several different putative binding sites, including the ATPase domain known to bind small fragments like tetrapeptide and bicyclic aromatics [17]. One preferred conformation of B02 showed motif 2 (3-pyridyl) occupying the same cleft that accommodated aromatic groups, like the phenylalanine side chain of Phe-His-Thr-Ala (Figure 2). Motifs 1 and 3 instead spread-eagled across the shallow hydrophobic entrance to the cleft with the charged residue D187 nearby. The cleft was surrounded by hydrophobic residues (L104, M158, I160, A190, A192, L203, A207, L219). A second shallow indentation close to motif 3, accommodating the threonine side chain of the tetrapeptide in the crystal structure with a truncated RAD51 [17], is formed by hydrophobic residues (F166, P168, L171, V185, L186, V189). These features were used to design our compound library in this report.

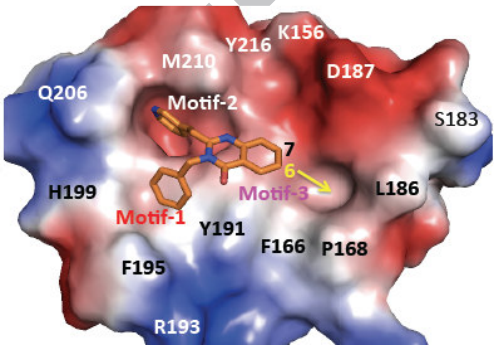

Figure 2. Docking of B02 in the ATPase domain of a homology model of human RAD51.

Ligands were synthesized, as shown in Scheme 1, to allow for independent optimisation of the three motifs (Scheme 1). Two general strategies were implemented, both involving the incorporation of motif 1 (R^1) onto initial motif 3 (**D** to **E**, or **H** to **I**). The difference between early (**A** to **B**) or late (**I** to **F**) stages allowed incorporation of motif 2 (R^2). The synthetic pathways were chosen so as to maintain the common intermediate as late as possible for structural diversification. To introduce motif 1 (R^1 in **F**), the common intermediate acid **D** (e.g. R^2 = 3-pyridyl) was assembled by coupling ethyl anthranilate **A** with the corresponding acyl chloride, followed by ester hydrolysis. Depending on the availability of the building blocks, the cinnamide analogues (**B**) were also constructed by Heck coupling of the corresponding aromatic bromide with acrylamide **C**. After introducing motif 1 as an amine through amide coupling (**D** to **E**), the intermediates were cyclized under mild dehydration conditions with iodine and hexamethyldisilazine[18] to give the desired quinazolinone products (**F**). In this way, one series of compounds incorporated alkyl and cycloalkyl substituents (**1**–**8**), and another series contained substituted aromatics with a variable spacer –(CH_2)n– (n =0-2, **9**–**27**). The latter series was designed to optimally target residues F195 and Y191 through pi-interactions. Various substituents, such as halogen, hydroxy, amino and its precursor nitro, carboxylate and acetamide were incorporated to improve properties or polar interactions.

Motif 2 (R^2 in **F**, R^1 = 4-chlorobenzyl) was assembled using either a similar linear process (**A** to **E** to **F**), or more efficiently from common intermediate 2-methylquinazolinone **I** through one-step divergent enamine-aldehyde coupling (**I** to **J** to **F**). A one-pot synthesis from anthranilic acid **G** to 2-methylquinazolinone **I**, through the mixed anhydride 2-methyloxazinone **H**, was used to prepare variations in Motif 3 (R^3). To probe the shallow hydrophobic cleft where threonine of Phe-His-Thr-Ala bound (Figure 2), one amino group was introduced at position 6 of the quinazolinone core (**44**), which was further derivatized by either acylation (**45–51**) or guanidinylation (**52**).

The potency of ligands was assessed using immunofluorescent assay for their inhibition of DNA damage induced RAD51 foci formation (Figure 3), a critical property of RAD51 in HR. An initial modification at motif 1 (**1**–**17**) resulted in promising compounds, with both saturated cyclohexylmethyl (**6**) and 4-chlorobenzyl (**17**) analogues displaying improved inhibition of RAD51 foci formation. One methylene spacer shorter (**5** *vs* **6**) or longer (**10** *vs* B02) reduced the potency of RAD51 functional inhibition. Restricting rotation (indane **11**) or introducing potential charged isosteres, such as morpholine (**7**–**8**) or pyridine to replace benzene (**12**–**14**), all reduced efficacy. Smaller alkanes (**1**–**4**) also displayed reduced activity. Varying spacer length in compound **17**, with one methylene unit shorter (**15**) or longer (**16**), did not improve activity and indicated optimal positioning of the aromatic ring in **17**. Of the substituted benzyl series, fluoro (**18**–**20**), nitro (**21**–**22**) and *p*-hydroxy (**23**) analogues showed comparable activity. A polar substrate, such as *p*-acetamidomethyl (**24**) and carboxylic acid (**25**–**26**), were detrimental, while 3,4-dichloro (**27**) conferred a slight improvement. This demonstrated that a hydrophobic interaction was important at this site.

Keeping motif 1 as 4-chlorobenzyl, any modifications at motif 2 apart from 3-pyridyl were detrimental, including its regioisomer 4-pyridyl (**36**), mono-amino substituted 3-pyridyl (**37**–**39**), and a series of mono-substituted (hydoxy, nitro or amino) phenyl (**28**–**35**). This suggested that there were limits to both the substituent size and the polar interaction, with only the 3-pyridyl moiety being effective at this site.

ACCEPTED MANUSCRIPT

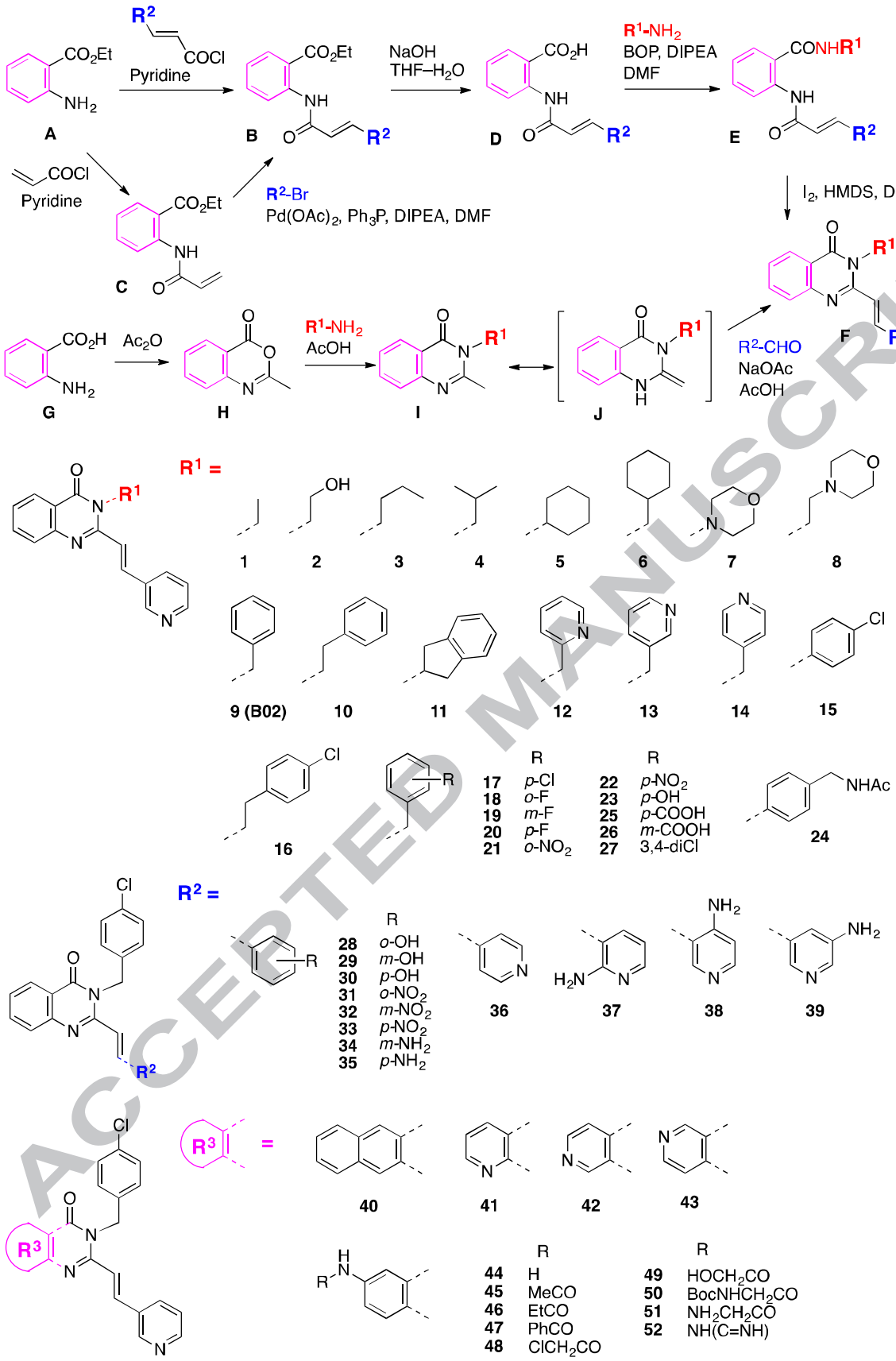

Scheme 1. Synthetic analogues of B02 and their preparation.

ACCEPTED MANUSCRIPT

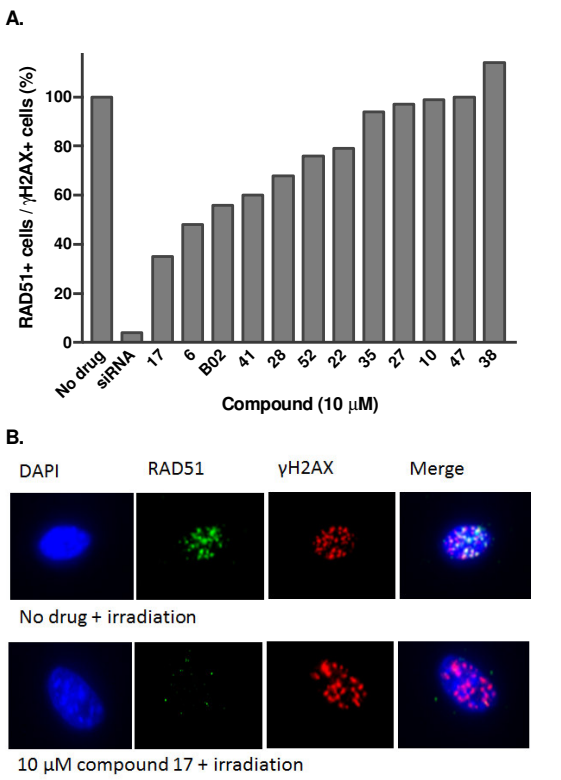

Figure 3. Inhibition of RAD51 foci formation following irradiation induced DNA damage by representative compounds. (A) The ratio of RAD51 positive cells/γH2AX positive cells was quantified by IF in MDA-MB-231 cells following treatment with 10 μM of each compound and exposure to 6 Gy irradiation. (B) Representative images show that **17** (10 μM) significantly inhibits DNA damage induced RAD51 foci formation with 6 Gy irradiation.

In motif 3, incorporating an extended pi-system (**40**) or a nitrogen isostere (**41**–**43**) led to similar or increased cytotoxicity. In particular, the 6-aza quinazolinone analogue (**43**) produced the greatest cytotoxicity. Surface plasmon resonance (SPR) and further profiling in different assays indicated ligands **43**, **48** and **51** were non-selective binders of several proteins. Overall, compound **17**, which elicited a favorable binding response representing 1:1 binding to RAD51 according to SPR, was notable for superior inhibition of DNA damage induced RAD51 foci formation.

Compound **17** was further investigated for sensitizing TNBC cell line MDA-MB-231 to irradiation. Combination of **17** and irradiation significantly reduced cell proliferation compared to **17** alone ($p<0.0005$) or B02 combined with irradiation ($p<0.05$, Figure 4). Compared with B02 for growth inhibition in a panel of six TNBC cell lines with varying levels of RAD51 expression (Figure 5), compound **17** was more potent than B02 ($IC_{50} \leq 13.7$ μM vs ≤ 89.1 μM) across all TNBC cell lines assessed. The differing sensitivity of TNBC cell lines to RAD51 inhibition is likely influenced by specific mutations contained by each cell line and compensatory activity of alternate DNA repair pathways in response to RAD51 inhibition [19]. We have previously shown that high RAD51 expressing MDA-MB-231 and MDA-MB-436 cells are almost entirely reliant on the HR pathway and show minimal non-homologous end joining (NHEJ) activity when HR is disrupted by RAD51 inhibition. We showed correlation of RAD51 expression and IC_{50} in these cell lines. In contrast, high RAD51 expressing HCC1937 increases NHEJ activity when RAD51 is inhibited [19]. We observed a slightly higher IC_{50} in this cell line. These differing sensitivity profiles to RAD51 inhibition are reflected in the IC_{50} values and the corresponding dose-curves (Supporting Information Figure S1). BT549 cells contain a PTEN mutation, which compromises HR activity [20], reflected by a gentler sloped dose curve in response to RAD51 inhibition. However, RAD51 inhibition was minimally toxic to normal breast epithelial cell line MCF10A which has unperturbed access to both HR and NHEJ repair pathways (IC_{50} ~ 48 μM, Table 1), suggesting a promising role in selectively inhibiting aggressive, metastatic breast cancer cells rather than normal cells.

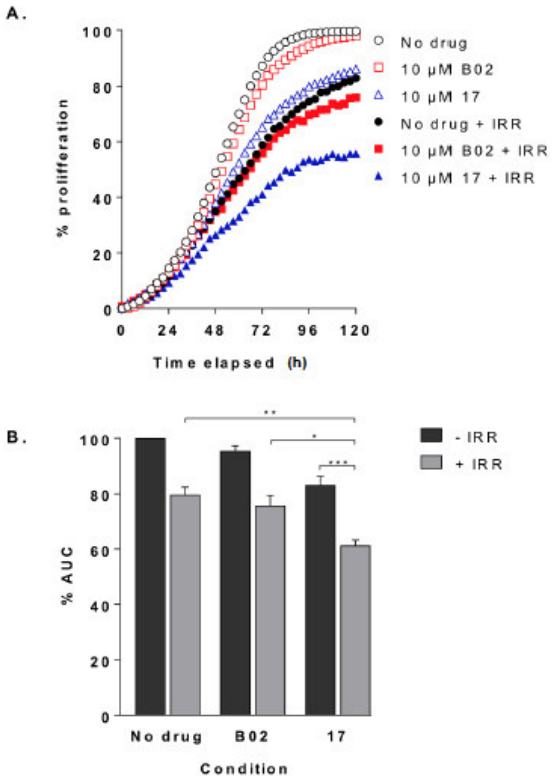

Figure 4. Effect of compound **17** on TNBC cell proliferation in combination with irradiation. (A) MDA-MB-231 cells were treated with 10 μM of B02 or **17** +/- 6 Gy irradiation and proliferation measured over a time course of 120 h. The graph shows the mean % proliferation from 3 independent experiments. (B) Area under the curve (AUC) was calculated from proliferation data. Treatment with 10 μM of **17** significantly sensitized cells to irradiation compared to no drug + irradiation ($p<0.005$), and was more highly significant than B02 plus irradiation ($p<0.05$).

In conclusion, by altering the known RAD51 inhibitor B02, we have identified a new cinnamylquinazoline compound (**17**) that shows enhanced cytotoxicity via RAD51. **17** effectively inhibits both RAD51 foci formation, in response to DNA damage, and proliferation of TNBC cell lines. Most importantly **17** sensitized aggressive metastatic TNBC to DNA damage induced by irradiation. Our data supports the principle of targeting the HR pathway, specifically RAD51, as a mechanism to sensitize aggressive cancer to DNA damaging treatments. Compound **17** will serve as a valuable research tool for developing combination therapies to overcome RAD51 driven resistance and relapse in a variety of cancers.

ACCEPTED MANUSCRIPT

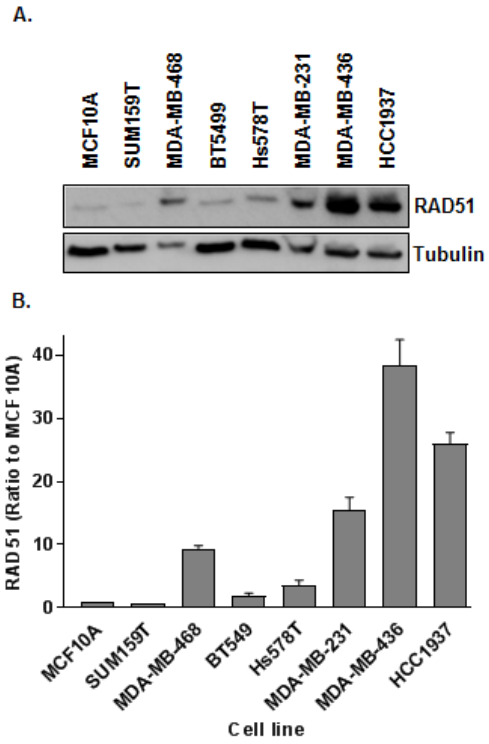

Figure 5. (A) Western blot analysis showing RAD51 expression in whole cell extracts from TNBC cell lines used in proliferation assay. (B) Bar graph represents the average result (± SEM) of two experiments with RAD51 expression normalised to MCF10A.

Table 1. Comparison of IC_{50} values for B02 and compound **17** in TNBC cell lines measured by MTS cell viability assay

Cell Line	IC_{50} ± SEM (μM)	
	B02	**17**
MCF10A[a]	47.7 ± 4.8	48.3 ± 4.8
SUM159T[b]	84.1 ± 1.6	5.5 ± 0.4 ***
MDA-MB-468[c]	10.2 ± 0.5	5.7 ± 0.5 **
BT549[d]	35.4 ± 1.0	6.4 ± 0.7 **
Hs578t[e]	9.6 ± 0.5	4.2 ± 0.5 *
MDA-MB-231[f]	11.1 ± 0.4	6.7 ± 0.4 *
MDA-MB-436[g]	5.7 ± 0.1	4.1 ± 0.1 **
HCC1937[h]	89.1 ± 5.7	13.7 ± 0.5 ***

* $p<0.05$, ** $p<0.005$ *** $p<0.0005$ based on two independent experiments.

[a]Non-tumourigenic epithelial cell line, [b]Infiltrating ductal carcinoma, [b]Adenocarcinoma, [c]Ductal carcinoma, [d]Carcinoma, [f]Adenocarcinoma, [g]Adenocarcinoma, [h]Ductal carcinoma.

Acknowledgments

We thank the National Health and Medical Research Council of Australia (NHMRC) for an SPR Fellowship to DPF (1117017), the National Breast Cancer Foundation (NBCF) for a Fellowship to APW (PF-13-12), the Queensland Emory Development Alliance for research support, and the ARC Centre of Excellence in Advanced Molecular Imaging (CE140100011).

References and Notes

1. Helleday, T. *Carcinogenesis* **2010**, *31*, 955.
2. Wiegmans, A. P.; Al-Ejeh, F.; Chee, N.; Yap, P.-Y.; Gorski, J. J.; Silva, L. D.; Bolderson, E.; Chenevix-Trench, G.; Anderson, R.; Simpson, P. T.; Lakhani, S. R.; Khanna, K. K. *Oncotarget* **2014**, *5.*, 3261.
3. King, H.; Payne, H.; Brend, T.; Patel, A.; Wright, A.; Englu, T.; Stead, L.; Wurdak, H.; Short, S. C. *Cancer Res.* **2015**, *75*, 3303.
4. Mitra, A.; Jameson, C.; Barbachano, Y.; Sanchez, L.; Kote□Jarai, Z.; Peock, S.; Sodha, N.; Bancroft, E.; Fletcher, A.; Cooper, C. *Histopathology* **2009**, *55*, 696.
5. Huang, F.; Mazin, A. V. *PLoS ONE* **2014**, *9*, e100993.
6. Huang, J.-W.; Wang, Y.; Dhillon, K. K.; Calses, P.; Villegas, E.; Mitchell, P. S.; Tewari, M.; Kemp, C. J.; Taniguchi, T. *Mol. Cancer Res.* **2013**, *11*, 1564.
7. Huang, F.; Mazina, O. M.; Zentner, I. J.; Cocklin, S.; Mazin, A. V. *J. Med. Chem.* **2012**, *55*, 3011.
8. Budke, B.; Logan, H. L.; Kalin, J. H.; Zelivianskaia, A. S.; McGuire, W. C.; Miller, L. L.; Stark, J. M.; Kozikowski, A. P.; Bishop, D. K.; Connell, P. P. *Nucleic Acids Res.* **2012**, *40*, 7347.
9. Budke, B.; Kalin, J. H.; Pawlowski, M.; Zelivianskaia, A. S.; Wu, M.; Kozikowski, A. P.; Connell, P. P. *J. Med. Chem.* **2012**, 254.
10. Lv, W.; Budke, B.; Pawlowski, M.; Connell, P. P.; Kozikowski, A. P. *J. Med. Chem.* **2016**.
11. Zhu, J.; Chen, H.; Guo, X. E.; Qiu, X.-L.; Hu, C.-M.; Chamberlin, A. R.; Lee, W.-H. *Eur. J. Med. Chem.* **2015**, *96*, 196.
12. Zhu, J.; Zhou, L.; Wu, G.; Konig, H.; Lin, X.; Li, G.; Qiu, X.-L.; Chen, C.-F.; Hu, C.-M.; Goldblatt, E.; Bhatia, R.; Chamberlin, A. R.; Chen, P.-L.; Lee, W.-H. *EMBO Mol. Med.* **2013**, *5*, 353.
13. Scott, D. E.; Coyne, A. G.; Venkitaraman, A.; Blundell, T. L.; Abell, C.; Hyvönen, M. *ChemMedChem* **2015**, *10*, 296.
14. Scott, D. E.; Marsh, M.; Blundell, T. L.; Abell, C.; Hyvonen, M. *FEBS Lett.* **2016**.
15. Huang, F.; Motlekar, N. A.; Burgwin, C. M.; Napper, A. D.; Diamond, S. L.; Mazin, A. V. *ACS Chem. Biol.* **2011**, *6*, 628.
16. Shin, D. S.; Pellegrini, L.; Daniels, D. S.; Yelent, B.; Craig, L.; Bates, D.; Yu, D. S.; Shivji, M. K.; Hitomi, C.; Arvai, A. S.; Volkmann, N.; Tsuruta, H.; Blundell, T. L.; Venkitaraman, A. R.; Tainer, J. A. *EMBO J.* **2003**, *22*, 4566.
17. Scott, D. E.; Ehebauer, M. T.; Pukala, T.; Marsh, M.; Blundell, T. L.; Venkitaraman, A. R.; Abell, C.; Hyvonen, M. *ChemBioChem* **2013**, *14*, 332.
18. Kshirsagar, U. A.; Mhaske, S. B.; Argade, N. P. *Tet. Lett.* **2007**, *48*, 3243.
19. Wiegmans, A. P.; Yap, P.-Y.; Ward, A.; Lim, Y. C.; Khanna, K. K. *Mol. Cancer Ther.* **2015**, *14*, 2321.
20. McEllin, B.; Camacho, C. V.; Mukherjee, B.; Hahm, B.; Tomimatsu, N.; Bachoo, R. M.; Burma, S. *Cancer Res.* **2010**, *70*, 5457.
21. *Spetral data of compound* **17**: m.p. 188–189 ºC (yellow powder, petroleum ether–EtOAc 5:1). ^{1}H NMR (DMSO-d_6, 600 MHz): δ 8.87 (d, 1H, J = 1.8 Hz, Py-H2), 8.56 (dd, 1H, J = 4.7, 1.3 Hz, Py-H6), 8.19 (dd, 1H, J = 7.9, 1.0 Hz, H5), 8.14 (ddd, 1H, J = 7.9, 1.8, 1.3 Hz, Py-H4), 7.90 (d, 1H, J = 15.4 Hz, *trans*-olefin-2′), 7.87 (ddd, 1H, J = 8.2, 7.1, 1.0 Hz, H7), 7.74 (d, 1H, J = 8.0 Hz, H8), 7.55 (ddd, 1H, J = 7.9, 7.1, 0.7 Hz, H6), 7.48 (d, 1H, J = 15.4 Hz, *trans*-olefin-1′), 7.45 (dd, 1H, J = 7.9, 4.7 Hz, Py-H5), 7.38 (d, 2H, J = 8.5 Hz, ClPh-H3/H5), 7.32 (d, 2H, J = 8.5 Hz, ClPh-H2/H6), 5.64 (s, 2H, NCH_2). ^{13}C NMR (DMSO-d_6, 150 MHz): δ 161.5 (C, C4), 151.6 (C, C2), 150.4 (CH, Py-C6), 149.6 (CH, Py-C2), 147.1 (C, C8a), 137.0 (CH, olefin-2′), 136.3 (C), 134.8 (CH, C7), 134.4 (CH, Py-C4), 132.0 (C), 130.8 (C), 128.7 (CH, ClPh-C3/C5), 128.6 (CH, ClPh-C2/C6), 127.2 (CH, C8), 126.9 (CH, C6), 126.6 (CH, C5), 123.4 (CH, Py-C5), 121.6 (CH, olefin-1′), 120.0 (C, C4a), 44.7 (CH_2, NCH_2). HPLC: t_R = 14.2 min (97% purity); MS: m/z 374 (100%), 376 (40%) $[M + H]^+$; HRMS: calcd for $C_{22}H_{17}ClN_3O^+$ $[M + H]^+$ 374.1055, found 374.1050.

ACCEPTED MANUSCRIPT

Supplementary Material

Synthetic procedures, compound characterization data (^{1}H and ^{13}C NMR, HRMS, HPLC), and assay conditions can be found in the online version.

ACCEPTED MANUSCRIPT

ACCEPTED MANUSCRIPT

Graphical Abstract

To create your abstract, type over the instructions in the template box below.
Fonts or abstract dimensions should not be changed or altered.

Quinazolinone derivatives as inhibitors of homologous recombinase RAD51

Leave this area blank for abstract info.

Ambber Ward[a], Lilong Dong[b], Jonathan M. Harris[c], Kum Kum Khanna[d], Fares Al-Ejeh[a], David P. Fairlie[b,e], Adrian P. Wiegmans[a,f*] and Ligong Liu[b,e*]

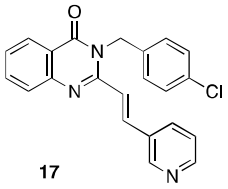

17

Compound **17** inhibits RAD51 foci formation and sensitizes aggressive breast cancer cells to DNA damage

ACCEPTED MANUSCRIPT